

# Applying full-azimuth depth processing in the Local Angle Domain for Frequency Absorption versus Azimuth) (FAVAz) analysis to predict permeable, oil-saturated fractures

Alexander Inozemtsev<sup>1\*</sup>, Gali Dekel<sup>1</sup>, Zvi Koren<sup>1</sup> and Alexander Galkin<sup>2</sup> present a study of carbonate reservoirs in an oil field in the Middle Volga region of Russia and suggests a workflow based on imaging and processing in the Local Angle Domain to predict prospective areas of oil-saturated fractured reservoirs.

## Introduction

Predicting the permeability of fractured reservoirs is valuable for both reservoir assessment and drilling planning. Characterization of such systems requires advanced amplitude analysis, mainly based on seismic imaging results of the recorded wavefield. A significant amount of work has been done on the subject over the past few decades.

Thomsen (1995) showed the effect of seismic amplitude variations for different fractured media. Pisetsky and Fedorov (1998) showed the influence of the size of cracks and the seismic wave length on the change of reflection coefficient. Rüger (1998) used the Zoeppritz equation to formalize the reflection coefficient variation as a function of the wavefront azimuthal direction with respect to the fracture azimuth. An approximation of the latter by Tsvankin and Grechka (1998) became the basis for AVAz inversion analysis.

Studies have also been performed on frequency absorption properties of fluid-saturated and dry fractured layers. Goloshubin (2002) observed that reflections are stronger for fluid-saturated fractured layers than for dry fractured layers at low-frequency ranges.

Geek (2008) studied high-frequency absorption vs. wavefront azimuth for dry fractures in the acoustic frequency range for P-waves, and showed that the absorption is insensitive to the azimuth for S-waves. Kozlov (2006) made a comprehensive generalization of the physics of frequency absorption effects in the case of dry and fluid-saturated fractures. In his study he showed that in fractured reservoirs, high fluid permeability has an observable effect of absorption of the low-frequency spectral range for reflected P-waves. This observation was also noted in several exploration areas of Western Siberia (Upper and Middle Jurassic deposits, Davydova, 2004).

Despite the research detailed above, predicting and delineating oil-saturated fracture systems using low-frequency absorption analysis has not yet become a standard practice in the industry. This is in large part due to the approximation

made by standard processing and imaging methods in creating azimuthal data. To make this process more effective, a true amplitude full-azimuth imaging procedure that decomposes the fully recorded seismic wavefield in the local angle domain is required. This procedure is carried out in-situ, in the depth migrated domain, preserving both reflection azimuth and structural azimuth. Such a technology is the ideal solution for extracting the main faults, building the Structural Tectonic Skeleton (STS), exposing the main fracture orientation, and eventually measuring anisotropic frequency absorption effects. This paper presents a study of carbonate reservoirs in an oil field in the Middle Volga region of Russia, and suggests a workflow based on imaging and processing in the Local Angle Domain to predict prospective areas of oil-saturated permeable fractured reservoirs.

## Workflow steps

Our workflow comprised the following steps:

1. Time domain pre-processing with preservation of amplitudes, spectrum and signal waveform.
2. Anisotropic (TTI) velocity model building.
3. Model-based 3D ray tracing simulation to study the full-azimuth illumination of the targeted region, taking into account transverse isotropy with tilted axis of symmetry (TTI), to estimate data reliability for full-azimuth studies.
4. Full-azimuth Local Angle Domain (LAD) migration, producing full-azimuth directional gathers (DG) and reflection gathers (RG).
  - Migration Aperture: 4000 m
  - Maximum half-opening angle at the top of the target horizon: 40° (RG)
  - Maximum dip: 80° (DG)
5. Extraction of information from the DG on the dip and azimuth of reflecting subsurface objects and heterogeneities.
6. Separation of the wavefield in the DG into specular reflection and diffraction components (diffraction imaging).

<sup>1</sup> Emerson Automation Solutions | <sup>2</sup>JSC 'ZPG'

\* Corresponding author, E-mail: Alexander.Inozemtsev@emerson.com

7. Azimuthally residual moveout (RMO) analysis for obtaining fast and slow normal moveout (NMO) velocities and the azimuth of the fast NMO velocity (referred to as velocity vs. azimuth [VVAZ] analysis).
8. Generalized Dix-type inversion to convert the global effective NMO parameters (ellipse) to local interval parameters (assuming transverse isotropy with a horizontal system of co-ordinates [HTI]).
9. Amplitude vs. azimuth (AVAZ) analysis to obtain fracture density and direction of the HTI axis of symmetry.
10. Study of frequency absorption as a function of the azimuth (FAVAz analysis).
11. Based on the FAVAz analysis, estimation of frequency absorption intensity (FAI) and prediction of permeable fracturing.
12. Integrated interpretation of AVAz and FAVAz analysis results to predict prospective zones of oil-saturated permeable fractured reservoirs.

### Main field parameters

1. Source: Vibroseis
2. Full-azimuth acquisition with maximum acquisition fold: 100
3. Source frequency spectrum: 12-100 Hz
4. Ratio of the length and width of the shot-receiver recording pattern: 0.9 (approximately a full-azimuth acquisition pattern)

### Result analysis

Figure 1 shows the central part of the geological section of the carbonate reservoirs, including a barrier reef. These are complex reservoirs with hard-to-recover hydrocarbon reserves deposited in complex geological conditions. This figure shows images obtained by Kirchhoff migration (left) and LAD migration (right). The complexity of the reservoir requires images of high

resolution and quality with better exposure of the reflecting boundaries, in order to build a structural skeleton. Image comparisons of Kirchhoff and Local Angle Domain migrations reveal higher structural detail and resolution in the LAD migration.

In Figure 2, the structural tectonic framework of the LAD image is merged with the HTI anisotropic intensity obtained with the AVAz analysis. This combination makes it easy to understand the general development of the fractures, taking into account the main macro faults and structural boundaries. It also helps to identify the areas with the most drilling potential in the fractured sections of the reservoir. It should be noted that the main anomalies are confined to faults or individual blocks. In general, the reservoir is confined by subvertical and inclined faults and has a block structure.

Figure 3 shows an example of the geometry and distribution of meso fractures in a geological section (A) vis-a-vis macro faults in the seismic section (B). The image on the left shows the fracture densities for different lithologies (marl below, siltstone above). Variations in fracture density are correlated to changes in lithology, where the fracture density is 10 times higher in the marl than in the mudstones. Slight changes in their dip are also noted. The fracture density is apparently dependent on the lithology (more often in marls, less in mudstones) and on the amplitude and direction of one-sided stress in the geological time interval when the fractures were formed. The seismic image on the right shows a merged section of the structural-tectonic skeleton (STS) and HTI intensity. This shows a similar picture to the inclined system of macro faults. Note that the increased HTI intensity is, to an extent, confined and defined by the STS.

Figure 4 shows the main fault imaging achieved using poststack (A) and prestack (B) domain-based techniques, on a depth slice at the top of the fractured reservoir. The poststack domain-based technique uses the Coherence Cube attribute

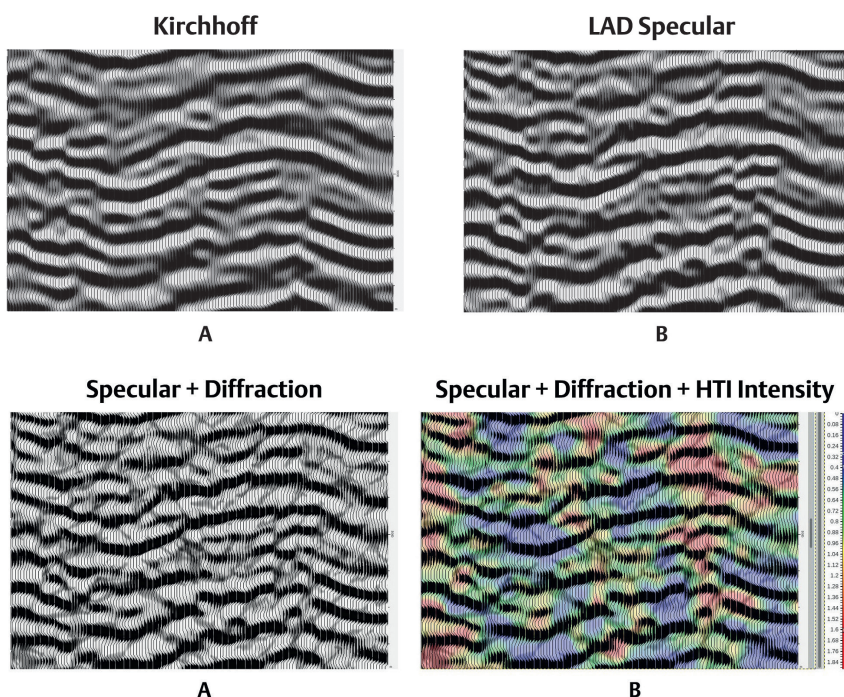
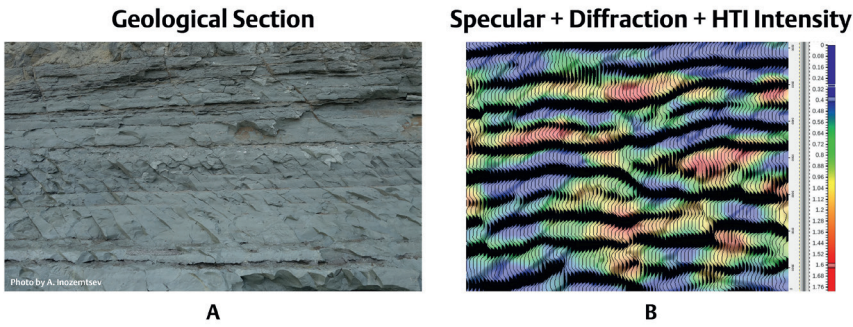
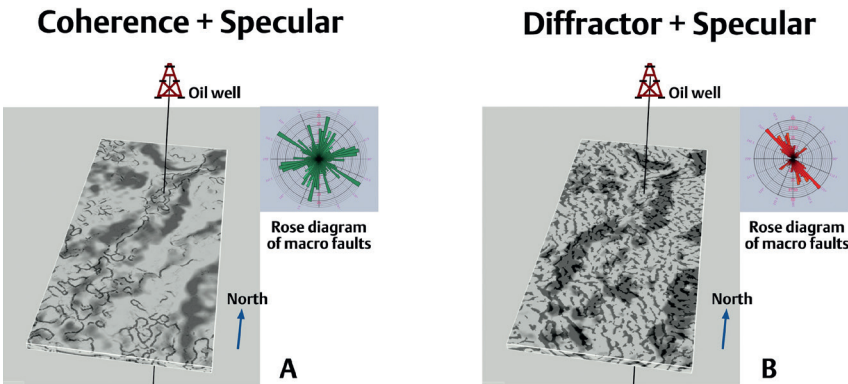


Figure 1 Comparison of depth images: A – PSDM Kirchhoff, B – LAD migration.

Figure 2 Seismic image of the structural-tectonic skeleton (A). Seismic merge imaging of the HTI intensity (AVAz inversion) inside the structural-tectonic skeleton (B).



**Figure 3** Comparison of the geometry and distribution features of the meso cracks on the geologic section (A) and macro faults on seismic data (B).



**Figure 4** Estimation of the azimuthal distribution of macro faults in the post-stack domain (A) and azimuthal distribution of macro-faults in the pre-stack domain (B) using diffraction filtering. The Devon 3 oil well penetrates a barrier reef with oil-saturated fractured reservoirs at a depth of 2998 m.

computed from the full stack volume, while the prestack domain-based technique uses diffraction filtering of the LAD directional gathers.

The Rose diagram next to each image shows the main azimuthal trends of the fault system. The fault trend is not definitive in image A, while image B shows three well-defined fault orientations. One such dominant trend is southeast to northwest. In addition, comparing the two images, it can be concluded that LAD prestack diffraction imaging enables a more reliable and

accurate determination of the position of the main faults (and thus regional stress) along which the barrier reef was formed, and is superior in that sense to the poststack Coherency Cube method.

Figure 5 (top figure) shows the inverse relationship of the extremes of the HTI anisotropy effect when changing the phase velocity (A) and amplitudes (B), depending on the azimuthal direction. The bottom figure shows that after the RMOz correction (A), the amplitude curve (B) remains almost unchanged. The QC factor (Relative Misfit Error [%]) of the deviation of real

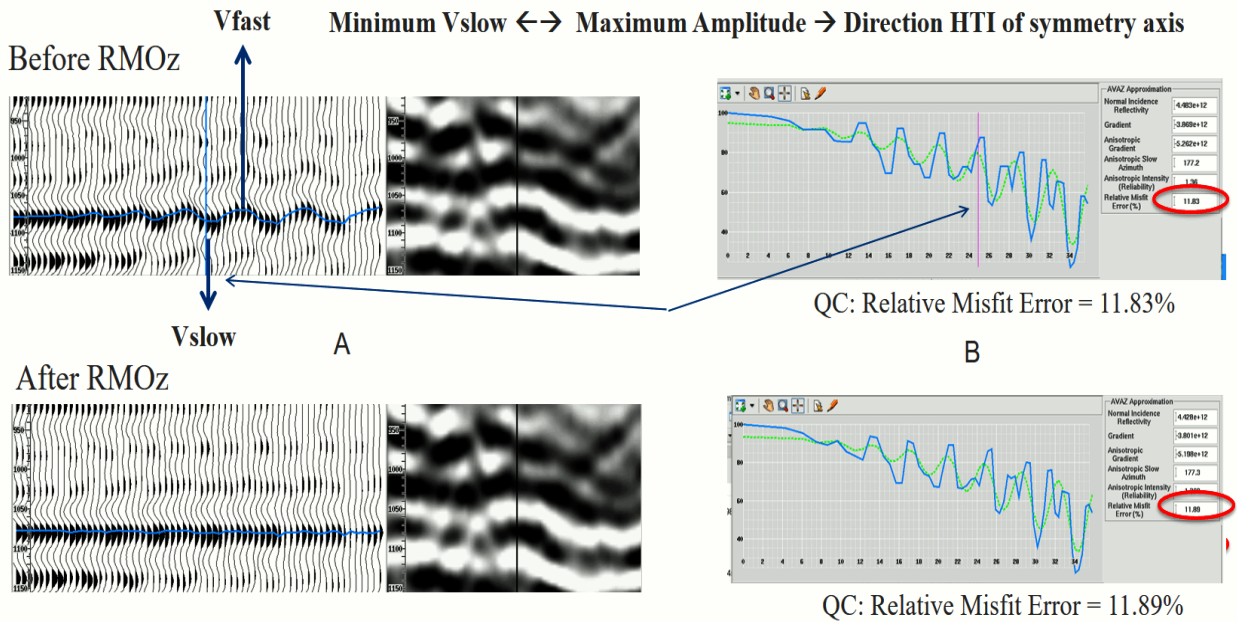


**Figure 5** Signature of HTI anisotropy effect observed by azimuthal changes in phase velocity (A) and amplitude (B) before and after azimuthal correction.

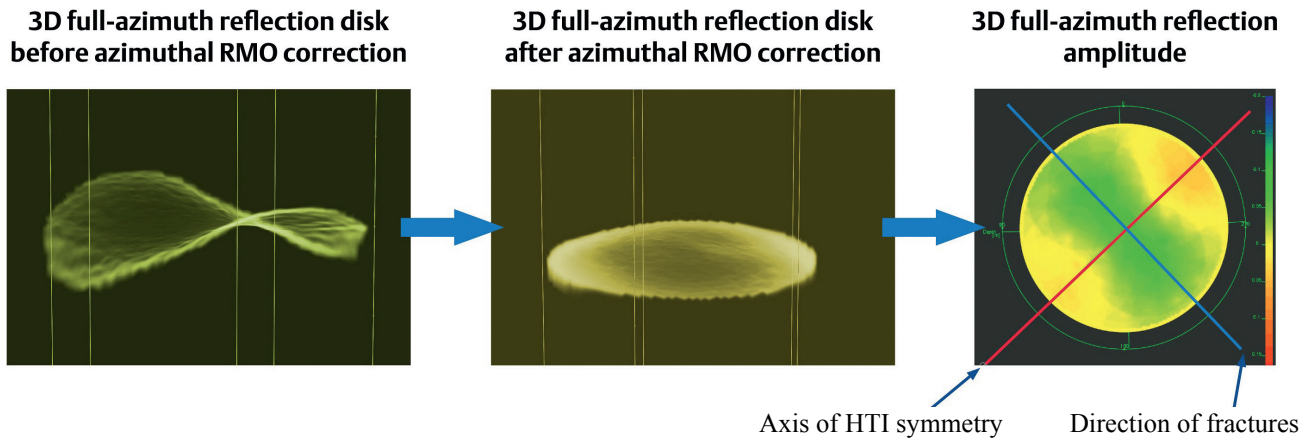


**Figure 6** Local registration of the HTI anisotropy effect by the criterion of phase velocity change (A) and amplitude variations (C), as a function of azimuth in the area of the oil-saturated well (top reservoir). Through the amplitude disk, it is easy to identify the direction of the axis of symmetry of the HTI – 130-140°, and correspondingly, the direction of the fracture – 40-50°.

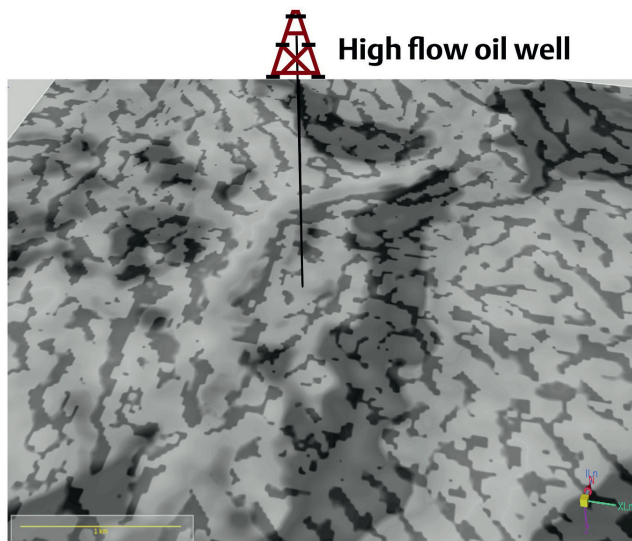


**Figure 7** 3D structural-tectonic image of the most promising part of the oil field. The image is extracted at the top of the carbonate reservoir (barrier reef) at a depth of 2998 meters.

amplitudes from the AVAz approximation) before and after the RMOz correction has changed only by 0.06%. This means that RMOz correction did not distort amplitude azimuthal behaviour.

Figure 6 shows a 3D angle–azimuth view of a LAD reflection surface before azimuthal RMO correction (A), after azimuthal

RMO correction (B), and a top view after azimuthal RMO correction (C). The reflection surface originates from the top of an oil-saturated reservoir in the vicinity of a highly productive well. The azimuthal orientation of the HTI axis of symmetry (130-140°) and of the orthogonal fracture system (40-50°) is easily detectable, as shown in image C.

### FAVAz analysis and results

Figure 7 shows a slice view of the 3D structural-tectonic frame of the LAD image in the vicinity of a highly saturated well at a depth of 2998 m (the top of the carbonate reservoir). The complex body of the reef is also observable. Macro faults are consistent with the reef body.

Figure 8 shows the seismic image of the structural tectonic frame interpretation of the LAD image, merged with HTI intensity (A) and with HTI axis symmetry (B) at the same location. The latter shows that the HTI symmetry axis orientation lies at azimuths 120-150°. This is consistent with the well log data measurements using the FMI method. A division into azimuthal sectors can now be applied for the benefit of Frequency Absorption vs. Azimuth analysis (FAVAz).

Figure 9 shows the sectored reflection gathers used for FAVAz along an inline section, in the vicinity of the oil-saturated well. The well marker corresponds to the top of the oil-saturated

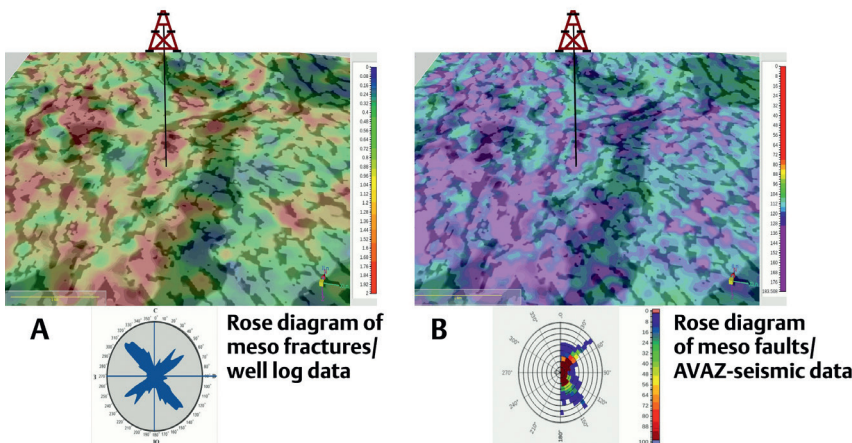


**Figure 8** Seismic image of STS and distribution of HTI intensity (A) and direction of HTI symmetric axis (B) in the most promising part of the oil field – the immediate vicinity of the oil-saturated well.

Azimuth stack sector + FA: 120-150°

Azimuth stack sector + FA: 30-60°

Full-azimuth stack + FA: 0-360°

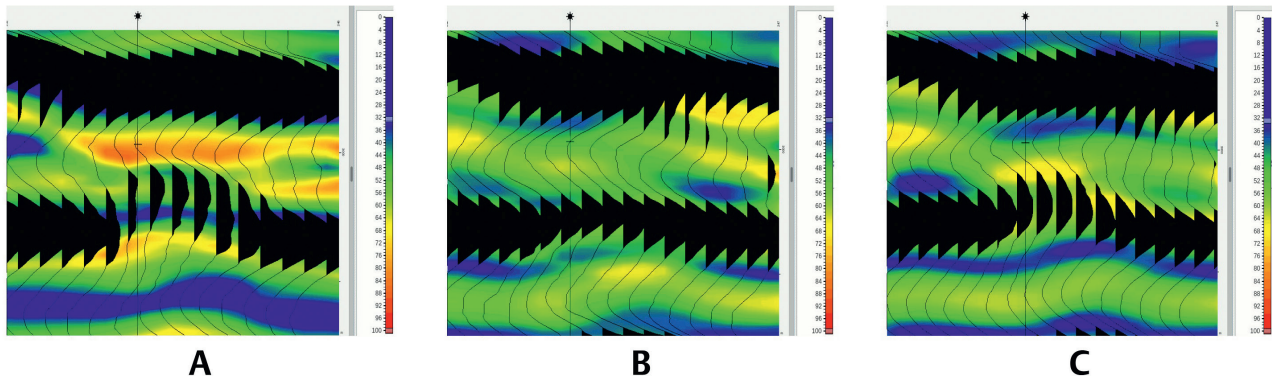


**Figure 9** Analysis of Frequency Absorption (FA), on azimuths (FAVAz) along an inline in the immediate vicinity of the oil-saturated well and in the vertical interval of the reservoir. The FA was estimated from the change in the dominant frequency. (A) Azimuth range of 120-150°. (B) Azimuth range of 30-60°. (C) Azimuth range of 0-360°.

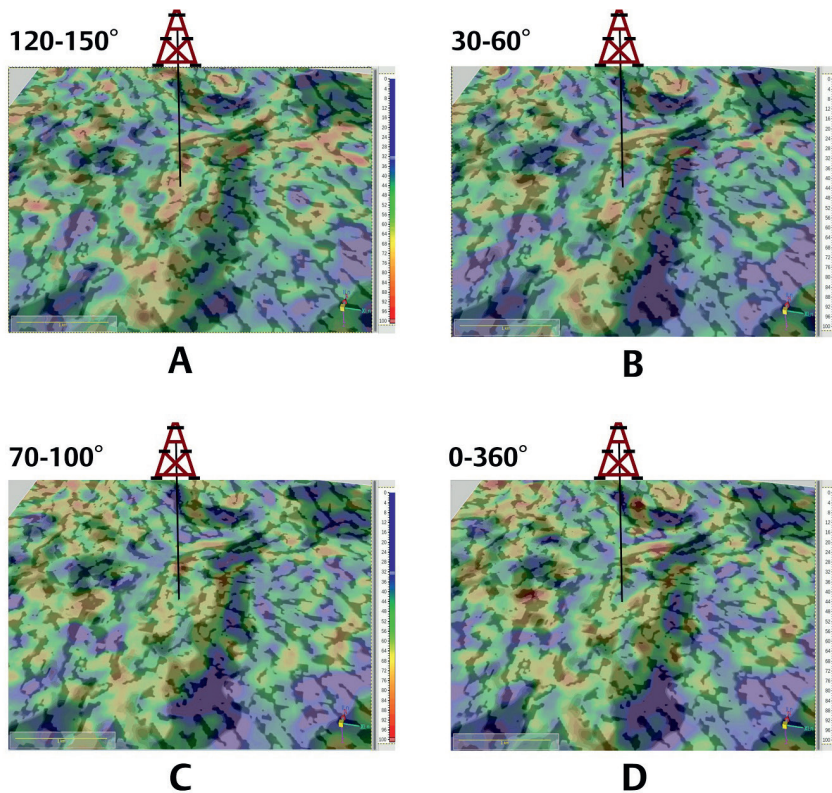


**Figure 10** FAVAz analysis in 3D view in the immediate vicinity of the oil-saturated well at a depth of top reservoir. (A) Azimuth range of 120-150°. (B) Azimuth range of 30-60°. (C) Azimuth range of 70-100°. (D) Azimuth range of 0-360°. The depth to the top of the carbonate reservoir is 2998 m.

reservoir. The frequency absorption intensity was estimated for each sector from the shift in the dominant frequency.

Analysis shows that in the azimuthal direction (120-150°) (B), coinciding with the direction of the HTI symmetry axis, there is a maximum absorption of the low-frequency components of the spectrum, expressed in the growth of high-frequency amplitudes (range of 60-80 Hz). In the azimuth direction of the sector (30-60°), minimal absorption of the low-frequency spectrum is observed, as the dominant frequencies are in the range of 20-50 Hz. In the case of a full azimuthal stack, we observe the average behaviour expressed in a less significant shift in the dominant frequency than that observed in either of the sectorized domains.

Figure 10 shows the seismic image of the STS merged with the dominant frequency distribution at different azimuth sectors; A - 120-150°, B - 30-60°, C - 70-100°, D - 0-360°.

Indeed, high-frequency amplitude regions dominate the azimuth sector of 120-150°, including the vicinity of the productive well. This corresponds to the effect of maximum absorption of the low-frequency component of the spectrum. This effect could be associated with the maximum amplitude of vibration on the fracture walls, and correspondingly, the maximum movement (friction) of oil along the permeable fractures to and from the pores.

Conversely, in the 30-60° sector, orthogonal to the HTI axis, the zones of high-frequency amplitudes are smaller. These are dominated by low frequencies, indicating the effect of minimal wavefront pressure due to vibrational motion on the fracture walls as the direction of the wave propagation coincides with the direction of the fractures. In the azimuth sector 70-100° (C), inclined at an angle to the direction of the fractures, a gradual

increase in the predominance of high frequencies is seen. In the full-azimuth version, 0-360°, one can see the distribution of the dominant frequency as an average of all azimuths.

Equivalent to HTI anisotropy intensity, it is possible to estimate the low-frequency absorption intensity (FAI) as the ratio of the FA values (the dominant frequency value) along the axis HTI symmetry, to the FA values orthogonal to the axis of HTI symmetry (or to the full-azimuth averaged absorption):  $FAI = FA(\underline{I}) / FA(II)$  or  $FAI = FA(\underline{I}) / FA(0-360)$ .

Figure 11 shows the HTI anisotropy intensity (A) and FAI (B) in the Seismic Image Structural Tectonic Skeleton (SI-STs) in an inline section around the well location.

The HTI intensity is more widely spread and captures both closed and permeable fractures. The FAI is more localized, both in the lateral and vertical directions. The FA and HTI intensity are generally correlated with each other, but non-linearly. Zones with a higher fracture density may contain fewer permeable fractures. Thus, the FAI is a direct indicator of permeable fractures (usually oil-saturated). The productive well passes through the maximum values of both HTI intensity and FAI.

We note that anomalous FAI zones are adjacent and confined by macro faults that make up the diffraction component. The

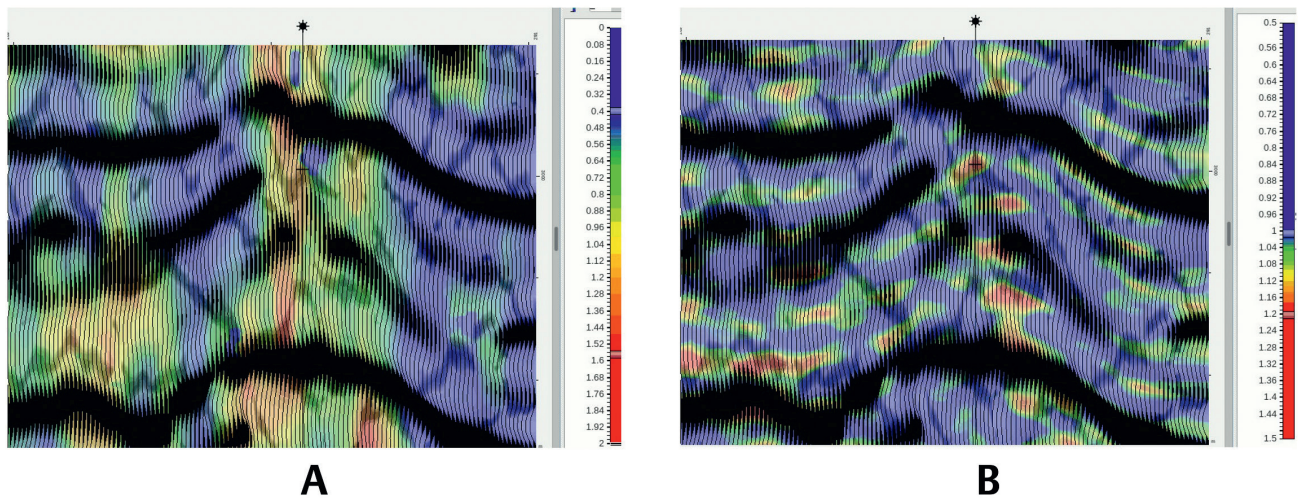
dip angles of faults are 30-40° relative to the vertical axis. This combination of structural and tectonic elements forms a structural-tectonic oil trap.

Figure 12 shows the HTI anisotropy intensity (A) and frequency absorption intensity (FA intensity) (B) in the SI-STs at the depth slice around the well location at the top of the oil-saturated reservoir.

In the vicinity of the productive well, the anomalous values of the FAI (B) form a narrower region than the HTI intensity (A). This is because the FAI is associated with open (or permeable) fractures, while HTI intensity is associated with general fractures (open or closed). This is another indication that FAI might be better for predicting and delineating such systems. Further insight could be gained by looking at the relation between them using crossplots.

In Figure 13, crossplots are generated between the HTI anisotropic intensity and FAI and prediction of the prospective zones.

From a crossplot of the correlated volumes of HTI fracture intensity and the computed FA attributes, anomalous points are located in the upper right-hand corner of the crossplot that are clearly separated from the background values of the lithological



**Figure 11** Comparison of the distribution of the HTI anisotropy intensity (reliability) (A) and the FA intensity (FAI) (B) in the SI-STs of the carbonate reservoir in the vicinity of the oil-saturated well. Along inline section.

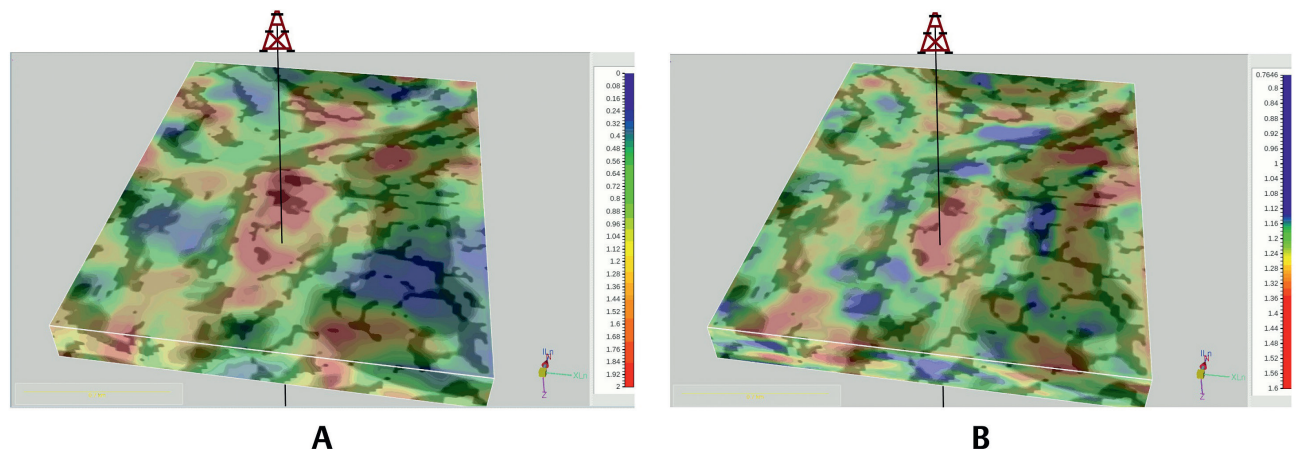


**Figure 12** Comparison of the distribution of the HTI anisotropy intensity (reliability) (A) and the FA intensity (FAI) (B) in the SI-STs of the carbonate reservoir in the vicinity of the oil-saturated well. The depth to the top of the carbonate reservoir is 2998 m.

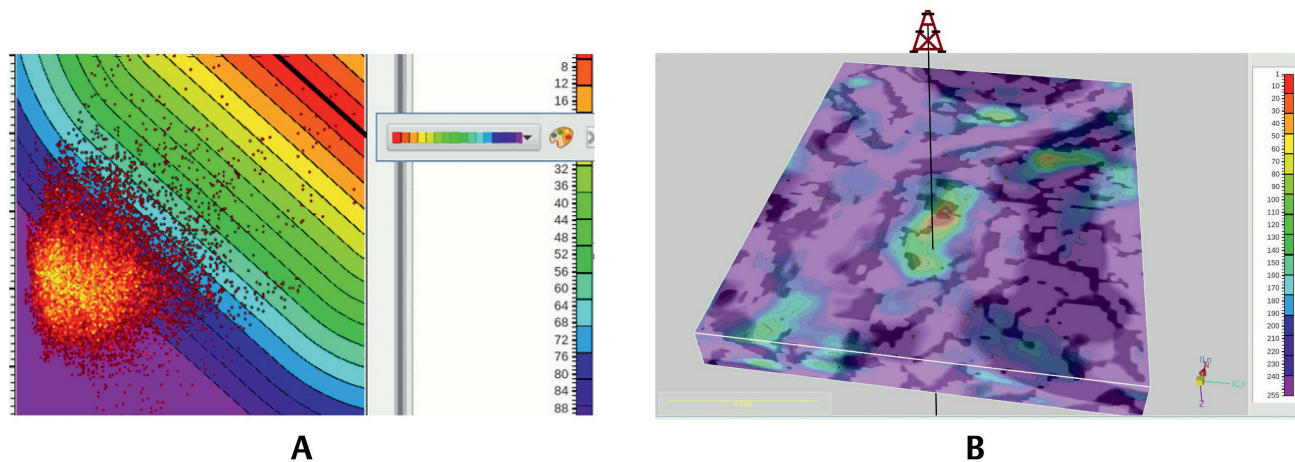


**Figure 13** Predicting prospective drilling zones based on cross-correlation between HTI Intensity and FAI (A) Crossplot between the attributes of HTI Intensity and FAI and color-coded version of the selection of abnormal points. (B) Marking (prediction) of anomalous points associated with permeable fracturing (oil saturation) in the 3D volume inside SI-STs.

trend. Anomalous points are associated with the most promising areas in terms of open (permeable) oil-saturated fractures. Colour marking of these points in the seismic image SI-STs allows selection of the most promising areas. This information is important both for drilling new production wells and for specifying the permeable zones when building hydrodynamic models.

### Conclusions

We have demonstrated new possibilities for predicting zones of permeable fractures using full-azimuth LAD technology. Using the processing workflow described above, including FAVAz analysis, it is possible to study not only the effects of HTI anisotropy associated with common fracturing, but also the subtler effects of azimuthal anisotropy associated with frequency absorption of reflected seismic signals in permeable fractured reservoirs. It is thus possible to reliably assign low-frequency absorption effects to open permeable fractures, which are usually associated with oil saturation. AVAz attributes give a more general picture of fracturing, including open and closed fractures. FAI, on the other hand, is a direct indicator of permeable fracturing. Crossplotting between the attributes of HTI intensity and FA significantly improves reliability when predicting oil-saturated permeable fractured zones for operational drilling tasks, and for building more accurate hydrodynamic models.

### Acknowledgements

The authors are grateful to the management of JSC ‘ZPG’ and Sintez for the opportunity to evaluate new Paradigm technologies using their data.

### References

- Canning, A. and Malkin, A. [2009]. Azimuthal AVA Analysis Using Full-Azimuth 3D Angle Gathers. *SEG Annual International Meeting*, Expanded Abstracts.
- Davydova, E.A. [2005]. Which side of seismic frequency band is most sensitive to hydraulic connectivity? *EAGE Annual Conference & Exhibition*, Expanded Abstracts.
- De Ribet, B., Yelin, G., Serfaty, Y., Chase, D., Kelvin, R. and Koren, Z. [2017]. High resolution diffraction imaging for reliable interpretation of fracture systems. *First Break*, **35**, 43-37.
- Geek, L.D. [2008]. Methods for studying cracks and pores of rocks based on acoustic logging data. Physical mesomechanics. *Proceedings of SB RAN*, 67-73.
- Goloshubin, G., Korneev, V. and Vingalov, V. [2002]. Seismic low-frequency effects from oil-saturated reservoir zones, *SEG Annual International Meeting*, Expanded Abstracts, 1813-1816.
- Grechka, V., and Tsvankin, I. [1998]. 3D description of normal moveout in anisotropic media. *Geophysics*, **63**, 1079-1092.
- Inozemtsev, A., Koren, Z. and Galkin, A. [2017]. Applying full-azimuth depth imaging in the local angle domain to delineate hard-to-recover hydrocarbon reserves. *First Break*, **35** (10), 49-58.
- Koren, Z. and Ravve, I. [2011]. Full-azimuth Subsurface Angle Domain Wavefield Decomposition and Imaging. *Geophysics*, **76** (1), P S1-S13.
- Kozlov, E.A. [2006]. *Models of the environment in exploration seismology*. GERS Publishing Ent.
- Pisetskiy, V.B. and Fedorov, Y.N. [1998]. *Dynamic-fluid method of forecasting and analysis of oil and gas deposits by seismic data*. Collection of scientific works of the Shpilman centre.
- Rüger, A. [1998]. Variation of P-wave reflectivity with offset and azimuth in anisotropic media, 1998. *Geophysics*, **63** (3), 935-947.
- Thomsen, L. [1995]. Elastic anisotropy due to aligned cracks on porous rock. *Geophysical Prospecting*, **43**, 805-830.

